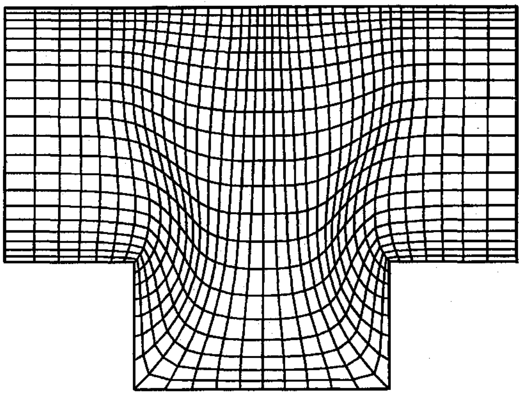

Fig. 2 Grid distribution for a channel with cavity (38 × 20), generated by proposed method starting from the lower and top boundaries, where the angle smoother (ω_q = 0.9) is applied twice.

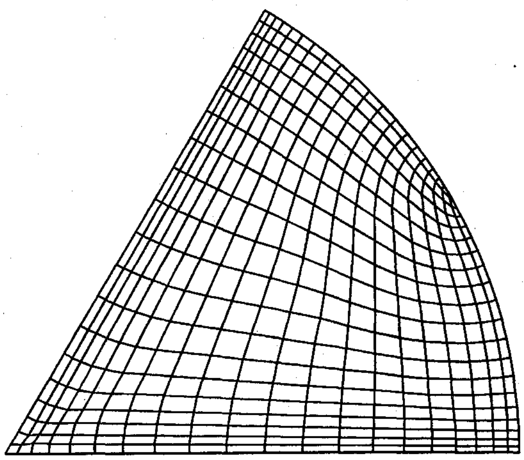

Fig. 3 Grid distribution in a 60-deg sector (20 × 20), generated by the proposed method starting from all of the boundaries, where the angle smoother (ω_q = 0.9) is applied three times.

the entire domain, and the convex and concave corners along the bottom boundary do not cause any trouble.

The second example for a region with enclosed boundaries is a 60-deg sector region. The result of the proposed method with the angle smoother applied three times ($\omega_q = 0.9$) is shown in Fig. 3 (20 × 20), where approximate grid orthogonality is preserved very well in the interior region. In the region around the flattened corner, the angle smoother makes the grid line incline to the flattened corner so that the resulting grid is smoothly distributed.

Conclusions

Cordova and Barth's grid generation method solving the hyperbolic partial differential equation is successfully extended to problems with enclosed boundaries. The open boundary constraint is partially removed by properly prescribing the unknown grid level via a simple algebraic grid generator equipped with the angle smoother and using corrections from the side boundaries. Several examples show that the proposed method preserves approximate grid orthogonality around all of the desired boundaries and provides smooth grid distribution over the entire domain.

Acknowledgment

This work was supported by the National Science Council of Taiwan under Grant 84-2212-E006-090.

References

[1]Thompson, J. F., Thames, F. C., and Mastin, C. W., "Boundary-Fitted Coordinate Systems for Numerical Solution of Partial Differential Equations—A Review," *Journal of Computational Physics*, Vol. 47, 1982, pp. 1–108.

[2]Nakamura, S., "Marching Grid Generation Using Parabolic Partial Differential Equations," *Numerical Grid Generation*, edited by J. F., Thompson, Elsevier, Oxford, England, UK, 1982, pp. 775–786.

[3]Noack, R. W., "Inviscid Flow Field Analysis of Maneuvering Hypersonic Vehicle Using the SCM Formulation and Parabolic Grid Generation," AIAA Paper 85-1682, July 1985.

[4]Hodge, J. K., Leone, S. A., and McCarty, R. L., "Noniterative Parabolic Grid Generation for Parabolized Equations," *AIAA Journal*, Vol. 25, No. 4, 1987, pp. 542–549.

[5]Steger, J. L., and Chaussee, D. S., "Generation of Body-Fitted Coordinates Using Hyperbolic Partial Differential Equations," *SIAM Journal on Scientific and Statistical Computing* Vol. 1, No. 4, 1980, pp. 431–437.

[6]Hoffmann, K. A., Rutledge, W. H., and Rodi, P. E., "Hyperbolic Grid Generation Techniques for Blunt Body Configurations," *Numerical Grid Generation in Computational Fluid Mechanics '88*, edited by S. Sengupta, J. Häuser, P. R. Eiseman, and J. F. Thompson, Pineridge, Swansea, Wales, UK, 1988, pp. 147–156.

[7]Chan, W. M., and Steger, J. L., "Enhancements of a Three-Dimensional Hyperbolic Grid Generation Scheme," *Applied Mathematics and Computation*, Vol. 51, 1992, pp. 181–205.

[8]Tai, C. H., Yih, S. L., and Soong, C. Y., "A Novel Hyperbolic Grid Generation Procedure with Inherent Adaptive Dissipation," *Journal of Computational Physics*, Vol. 116, 1995, pp. 173–179.

[9]Jeng, Y. N., Shu, Y. L., and Lin, W. W., "On Grid Generation for Internal Flow Problems by Methods Solving Hyperbolic Equations," *Numerical Heat Transfer, Part B*, Vol. 27, 1995, pp. 43–61.

[10]Jeng, Y. N., and Shu, Y. L., "Grid Combination Method for Hyperbolic Grid Solver in Regions with Enclosed Boundaries," *AIAA Journal*, Vol. 33, No. 6, 1995, pp. 1152–1154.

[11]Liou, Y. C., and Jeng, Y. N., "The Algebraic Grid Front Marching Methods," *Numerical Heat Transfer, Part B*, Vol. 28, 1995, pp. 257–276.

[12]Jeng, Y. N., and Liou, Y. C., "The Parabolic Equation Method of Grid Generation for Enclosed Regions," *Numerical Heat Transfer, Part B* (to be published).

[13]Cordova, J. Q., and Barth, T. J., "Grid Generation for General 2-D Regions Using Hyperbolic Equations," AIAA Paper 88-0520, Jan. 1988.

Calculation of Interlaminar Stresses in Laminated Plates Using Walsh Transforms

Martin Crane* and J. T. Boyle†
University of Strathclyde,
Glasgow G1 1XQ, Scotland, United Kingdom

Nomenclature

A, B, D	= extensional/extensional, extensional/bending and bending/bending coupling terms, respectively
$B_{(m)}$	= mth order Walsh operational matrix for differentiation, $H_{(m)}^{-1}$
C_i	= Walsh coefficients
F	= two-dimensional matrix of Walsh coefficients, f_{ij}
$H_{(m)}$	= mth order Walsh operational matrix for integration
h	= plate thickness
l	= plate span in x direction
M^k	= kth laminar moment resultants
N^k	= kth laminar stress resultants
$\bar{Q}_{ij}^k$	= kth laminar transformed reduced stiffnesses
u, v, w	= displacements in x, y, z directions, respectively
$W_{(m)}$	= mth-order Walsh transform matrix
ϵ	= strains
κ	= curvatures
σ	= normal stresses
τ	= shear stresses
$\Phi_{(m)}$	= vector of ϕ_i functions for $i = 1, \ldots, m$
$\phi_i(x)$	= ith one-dimensional Walsh function in x

I. Introduction

SINCE their development in 1923 by Walsh,[1] Walsh functions have found wide applications in the field of engineering compu-

Received Feb. 8, 1995; revision received July 7, 1995; accepted for publication July 20, 1995.

*Research Fellow, Department of Mechanical Engineering.
†Professor, Department of Mechanical Engineering.

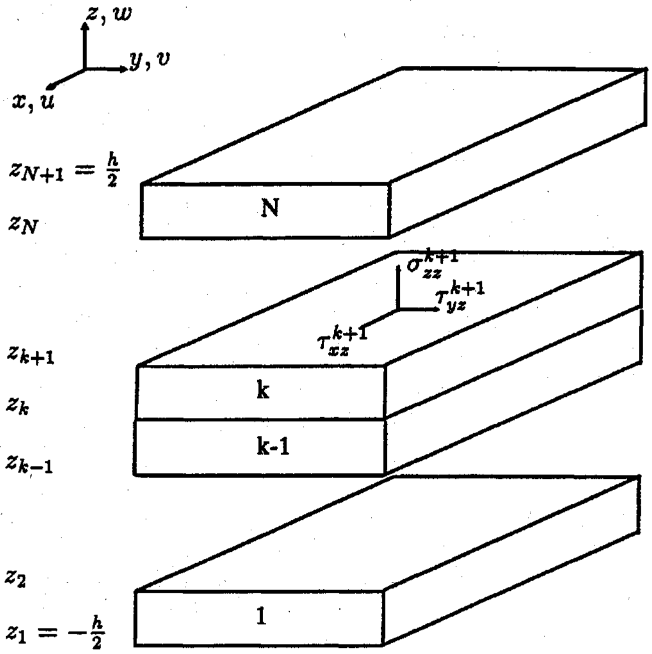

Fig. 1 Exploded view of a composite plate.

tation. In the past two decades, Walsh functions and transforms have been used in the numerical solution of many engineering problems (for example, see Refs. 2 and 3). Compared to this, the amount of attention devoted to the development of Walsh operational matrices for differentiation and integration is quite small indeed. LeVan et al.[4] originated the idea of such matrices for integration purposes, and this was extended by Sannuti[5] and Chen et al.[6] In this Note we further extend the use of operational matrices for differentiation to the calculation of the partial derivatives necessary for the determination of interlaminar stresses in laminates.

When a composite plate (such as that shown in exploded view in Fig. 1) is put in a state of stress, interlaminar stresses are induced that can often lead to catastrophic failure of the composite. It is obviously essential to know the location and extent of these stresses if composite materials are to be widely used in practice. As the interlaminar stresses can only be computed exactly when exact analytical solutions of the equilibrium equations of three-dimensional elasticity are available, approximate solutions must be relied on for the most part. To date, the majority of such approximate solutions to this problem have taken the form of so-called recontinuization involving interpolation of the displacement data from a finite element package. The purpose of this process is to improve the accuracy of the derivative results from the finite element displacement data. Byun and Kapania[7] (in addition to a bibliography on the problem) give examples using Chebyshev polynomials and a class of orthogonal polynomials (which can be generated for a given location of known data points) as these interpolation polynomials. In our Note, values for the interlaminar stresses calculated using a method based on Walsh transforms are compared with those from classical laminated plate theory (CPT) in a typical problem. This approach would allow enhanced postprocessing from conventional finite element CPT analysis if more advanced laminated plate elements were unavailable.

II. Walsh Operational Matrices

As has already been remarked, Walsh functions have been used extensively in the solution of differential equations. Corrington[2] set out the first 16 Walsh functions and the so-called Rademacher functions (sequency ordered rectangular orthonormal functions) from which they may be derived.

The Walsh approximation of an absolutely integrable function $g(t)$ for $0 \leq t \leq 1$ can be written as

$$g(t) \approx \sum_{i=0}^{n} C_i \phi_i(t) \tag{1}$$

where

$$C_i = \int_0^1 g(t)\phi_i(t)\,\mathrm{d}t$$

As with any set of orthogonal polynomials Walsh functions may be used to approximate an arbitrary function in two dimensions as follows:

$$f(x, y) = \mathbf{\Phi}^T_{(m)}(x)\mathbf{F}\mathbf{\Phi}_{(n)}(y) \tag{2}$$

where m and n are the order of the Walsh functions in the x and y directions, respectively,

$$\mathbf{\Phi}_{(m)}(x) = [\phi_1(x)\phi_2(x)\cdots\phi_m(x)]^T$$

$$\mathbf{\Phi}_{(n)}(y) = [\phi_1(y)\phi_2(y)\cdots\phi_n(y)]^T$$

$$F = \begin{bmatrix} f_{00} & f_{01} & \cdots & f_{0,n-1} \\ f_{10} & f_{11} & \cdots & f_{1,n-1} \\ \vdots & & & \vdots \\ f_{m-1,0} & f_{m-1,1} & \cdots & f_{m-1,n-1} \end{bmatrix}$$

with

$$f_{ij} = \int_0^1 \int_0^1 \phi_j(x) f(x, y)\phi_i(y)\,\mathrm{d}x\,\mathrm{d}y$$

One of the interesting properties of Walsh functions is that (since the integral of a Walsh function may be expressed as a Walsh series) a matrix may be derived for the integration process. The Walsh matrix for integration of m values in the time domain may be shown (cf. Ahner[8]) to be

$$\boldsymbol{H}_{(m)} = \frac{1}{m}\begin{bmatrix} \frac{1}{2} & 1 & \cdots & 1 \\ 0 & \frac{1}{2} & \cdots & 1 \\ \cdots & & & \cdots \\ 0 & 0 & \cdots & \frac{1}{2} \end{bmatrix}$$

The inverse of the $\boldsymbol{H}$ matrix with $m = 4$ here has been shown (cf. Chen et al.[6]) to be

$$\boldsymbol{B}_{(m)} = 4m\begin{bmatrix} \frac{1}{2} & -1 & 1 & -1 \\ 0 & \frac{1}{2} & -1 & 1 \\ 0 & 0 & \frac{1}{2} & -1 \\ 0 & 0 & 0 & \frac{1}{2} \end{bmatrix} \tag{3}$$

which is the order four Walsh operational matrix for differentiation.

Given a set of discrete functional values $\boldsymbol{P}_{ij}$ where the x value varies with the row and the y value with the column, derivatives can be evaluated in the following way:

$$\frac{\partial}{\partial x}\boldsymbol{P}_{ij} = \boldsymbol{P}_{ij,x} \approx \boldsymbol{B}_{(m)}\boldsymbol{P}_{(m\times n)} \tag{4}$$

$$\frac{\partial}{\partial y}\boldsymbol{P}_{ij} = \boldsymbol{P}_{ij,y} \approx \boldsymbol{P}_{(m\times n)}\boldsymbol{B}^T_{(n)} \tag{5}$$

$$\frac{\partial^2}{\partial x \partial y}\boldsymbol{P}_{ij} = \boldsymbol{P}_{ij,xy} \approx \boldsymbol{B}_{(m)}\boldsymbol{P}_{(m\times n)}\boldsymbol{B}^T_{(n\times n)} \tag{6}$$

and so forth.

Note that Walsh differential operators do not infallibly produce the derivative values of the matrix of values on which they are employed. As with all differencing schemes, numerical instabilities can be and are often produced in the differentiation process. These instabilities may be removed from the derivative matrix by a simple averaging process that may be automatically carried out after each derivative is calculated. This averaging involves taking a simple mean of four derivative matrix entries (i, j), $(i, j+1)$, $(i+1, j)$, and $(i+1, j+1)$ (for $i = 1, n-1$ in steps of 2). This eliminates the errors incurred in all circumstances at the cost of a reduction in the number of data points available by a factor of two. In addition, there is the minor problem that the method described for the evaluation of derivatives requires the values for the functional data to be available at certain point, the Walsh points. This need not be a problem, however, as the finite element displacement data may be interpolated using a variety of procedures (we found that the one described by Comlekci[9] was optimal) to give the requisite data.

III. Interlaminar Traction Equations

As already remarked, one of the motivations for the derivation of the given operational matrices is in the calculation of the interlaminar tractions $(\tau_{xz}^k, \tau_{yz}^k, \sigma_{zz}^k)$ (i.e., σ_{zz}^1 refers to the normal stress under the first layer). Walsh functions and transforms have been used very successfully in the past for problems involving nonlinear terms because the product of two Walsh functions is also a Walsh function (cf. Corrington[2]). As the interlaminar tractions are calculated from the equilibrium equations that contain nonlinear terms, this would seem to suggest that the use of a method based on Walsh function is appropriate. It has been shown by Byun and Kapania[7] that in the case of the symmetric laminated plate problem these tractions are related to the nodal displacements (u, v, w) by the following relations (derived from the three-dimensional elasticity equations with nonlinear terms retained):

$$\tau_{xz}^{k+1} = \tau_{xz}^1 - \left(\sum_{l=1}^{k} N_{x,x}^l + \sum_{l=1}^{k} N_{xy,y}^l\right) \tag{7}$$

$$\tau_{yz}^{k+1} = \tau_{yz}^1 - \left(\sum_{l=1}^{k} N_{xy,x}^l + \sum_{l=1}^{k} N_{y,y}^l\right) \tag{8}$$

$$\begin{aligned}\sigma_{zz}^{k+1} = \sigma_{zz}^1 &- \left(\sum_{l=1}^{k} M_{x,xx}^l + 2\sum_{l=1}^{k} M_{xy,xy}^l + \sum_{l=1}^{k} M_{y,yy}^l\right)\\ &- \left(w_{,xx}\sum_{l=1}^{k} N_x^l + 2w_{,xy}\sum_{l=1}^{k} N_{xy}^l + w_{,yy}\sum_{l=1}^{k} N_y^l\right)\\ &- z_{k+1}\left(\sum_{l=1}^{k} N_{x,xx}^l + 2\sum_{l=1}^{k} N_{xy,xy}^l + \sum_{l=1}^{k} N_{y,yy}^l\right)\end{aligned} \tag{9}$$

In Eq. (9) the lamina stress resultants N_i^k are given by

$$N_i^k = \sum_j \left[(z_{k+1} - z_k)\bar{Q}_{ij}^k \epsilon_j^0 + \frac{1}{2}(z_{k+1}^2 - z_k^2)\bar{Q}_{ij}^k \kappa_j\right] \qquad i, j = 1, 2, 6 \tag{10}$$

and the lamina moment resultants M_i^k are given by

$$M_i^k = \sum_j \left[\frac{1}{2}(z_{k+1}^2 - z_k^2)\bar{Q}_{ij}^k \epsilon_j^0 + \frac{1}{3}(z_{k+1}^3 - z_k^3)\bar{Q}_{ij}^k \kappa_j\right] \qquad i, j = 1, 2, 6 \tag{11}$$

where z_k is the z value at the kth layer and $\bar{Q}_{ij}^k$ are the transformed reduced stiffnesses of the kth layer.

The strains ϵ_j^0 are related to the displacements (u, v, w) by the following well-known relations:

$$\begin{aligned}\epsilon_1^0 &= u_{,x} + \tfrac{1}{2}w_{,x}^2\\ \epsilon_2^0 &= v_{,y} + \tfrac{1}{2}w_{,y}^2\\ \epsilon_6^0 &= u_{,y} + v_{,x} + w_{,x}w_{,y}\end{aligned} \tag{12}$$

and, similarly, the curvatures κ_j,

$$\begin{aligned}\kappa_1 &= -w_{,xx}\\ \kappa_2 &= -w_{,yy}\\ \kappa_6 &= -2w_{,xy}\end{aligned} \tag{13}$$

IV. Implementing the Interlaminar Stress Equations

A program has been written that calculates the interlaminar stresses σ_{zz}^{k+1} from Eq. (9). Because a large part of the computation in the program is taken up with calculation derivatives and because the order of the derivatives that must be computed is high, it is necessary 1) to have a reasonably large number of displacement data points n to start with (n will be reduced to $n/16$ by the end of the differentiation process as fourth-order derivatives have to be calculated) and 2) to make the differentiation process as efficient as possible in terms of computation expense.

As the displacement data is input in vector form (u, v, w), it is necessary to transform this into array format $(\boldsymbol{u}_{ij}, \boldsymbol{v}_{ij}, \boldsymbol{w}_{ij})$ where $i = 1, \ldots, n$, $j = 1, \ldots, m$. These subscripts will be omitted henceforth for clarity.

In this way, as has been shown, the Walsh approximation to the strain equations (13)

$$\begin{aligned}\epsilon_1^0 &= B_{(n)}u + \tfrac{1}{2}\left(B_{(n)}w\right)^2\\ \epsilon_2^0 &= vB_{(m)}^T + \tfrac{1}{2}\left(wB_{(m)}^T\right)^2\\ \epsilon_6^0 &= uB_{(m)}^T + B_{(n)}v + \left(B_{(n)}w\right)\left(wB_{(m)}^T\right)\end{aligned} \tag{14}$$

where the products and square terms are evaluated term by term. In the same way, the curvatures

$$\begin{aligned}\kappa_1 &= -B_{(n)}B_{(n)}w\\ \kappa_2 &= -wB_{(m)}^T B_{(m)}^T\\ \kappa_6 &= -2B_{(m)}wB_{(m)}^T\end{aligned} \tag{15}$$

Having thus calculated the strains and curvatures, the k individual lamina stress and moment resultants N_i^k and M_i^k may be found in a straightforward manner from Eqs. (10) and (11), respectively. To find the remaining terms in Eq. (9) it is necessary to take derivatives of these layer resultant matrices N_i^k and M_i^k and to multiply out term-by-term the values of $w_{,ij}$ by N_i^k. The individual summation terms that make up Eq. (9) can now be found by summing over the constituent layers.

V. Numerical Results from Sample Problems

To ascertain the accuracy of the method described for finding interlaminar stresses in composite materials, values for τ_{xz} and σ_{zz} are calculated for the case of cylindrical bending of a number of sample composite plates. The cylindrical bending problem is chosen because there is data available from a number of sources, and this data may be checked against CPT and elasticity solutions. The cylindrical bending problem has been examined by, among others, Pagano[10] and Pagano and Hatfield.[11] For ease of comparison we cite the results of Gaudenzi et al.[12]

The cases covered in this section are 1) unidirectional plate with fibers oriented in the x direction, 2) unsymmetrical composite plate (0/90 deg) with two layers of equal thickness, and 3) symmetrical composite plate (0/90/0 deg) with layers of equal thickness.

Table 1 Values of τ_{xz} and σ_{zz} for a single layer plate

z/h	τ_{xz} CLT[12]	τ_{xz} 64-pt Walsh	% error	σ_{zz} CLT[12]	σ_{zz} 64-pt Walsh	% error
−0.5	0	——	——	0	——	——
−0.3	1.22231	1.22214	1.4×10^{-2}	0.104	0.10394	5.4×10^{-2}
−0.1	1.83346	1.83322	1.3×10^{-2}	0.352	0.3518	5.6×10^{-2}
0.1	1.83346	1.83322	1.3×10^{-2}	0.648	0.64765	5.4×10^{-2}
0.3	1.22231	1.22214	1.4×10^{-2}	0.896	0.8955	5.6×10^{-2}
0.5	0	-1.5×10^{-16}	——	1	0.999466	5.3×10^{-2}

Table 2 Values of τ_{xz} and σ_{zz} for a two-layer 0/90 deg plate

z/h	τ_{xz} CLT[12]	τ_{xz} 64-pt Walsh	% error	σ_{zz} CLT[12]	σ_{zz} 64-pt Walsh	% error
−0.5	0	——	——	0	——	——
−0.4	1.75811	1.78448	1.5	0.07426	0.07537	1.47
−0.3	2.71856	2.75503	1.3	0.25528	0.25889	1.4
−0.2	2.88135	2.91165	1.0	0.48041	0.48666	1.3
−0.1	2.24649	2.25434	0.35	0.687	0.69477	1.1
0.0	0.81398	0.783079	−4.2	0.8124	0.81933	0.85
0.5	0	4.9×10^{-4}	——	1	0.9997	——

Table 3 Values of τ_{xz} and σ_{zz} for a three-layer 0/90/0 deg plate

z/h	τ_{xz} CLT[12]	τ_{xz} 64-pt Walsh	% error	σ_{zz} CLT[12]	σ_{zz} 64-pt Walsh	% error
−0.5	0	——	——	0	——	——
−0.367	0.915234	0.915184	-5.0×10^{-3}	0.05038	0.05035	-5.0×10^{-2}
−0.167	1.76007	1.760006	-3.6×10^{-3}	0.26879	0.26867	-4.5×10^{-2}
0.167	1.76007	1.760006	-3.6×10^{-3}	0.731209	0.73079	-5.7×10^{-2}
0.367	0.915234	0.915184	-5.0×10^{-3}	0.949621	0.94911	-5.5×10^{-2}
0.5	0	7.6×10^{-6}	——	1	0.999486	-5.1×10^{-2}

The laminate concerned is assumed to be simply supported at $x = 0$ and $x = l$, of infinite length and subjected to a sinusoidal load across the span of $q = q_0 \sin(\pi x/l)$ applied at $z = h/2$. For the purposes of postprocessing, it is assumed that the response to this load would be

$$u(x) = \left(Bq_0/Fp^3\right)\cos px, \qquad w(x) = \left(Aq_0/Fp^4\right)\sin px$$

where

$$F = AD - B^2 \quad \text{and} \quad (A, B, D) = \int_{-h/2}^{h/2} \bar{Q}^i_{11}(1, z, z^2)\,dz$$

For all of the cases, the following layer elastic constants apply:

$$E_1/E_2 = 25, \qquad G_{12}/E_2 = 0.5$$

$$G_{22}/E_2 = 0.2, \qquad \nu_{12} = \nu_{22} = 0.25$$

and the following dimensionless ratios are used:

$$p = l/h, \qquad \bar{\tau}_{xz} = \tau_{xz}/q_0, \qquad \bar{\sigma}_{zz} = \sigma_{zz}/q_0$$

The numerical results for the values of the interlaminar normal and shear stresses for the three examples described are shown in Tables 1–3. It can be seen from these tables that the values for the stresses calculated using the Walsh transform method correspond very well with those predicted by classical plate theory (as tabulated by Gaudenzi et al.[12] The values for those cases in which there is symmetry about the central axis (cases 1 and 3) are better than the asymmetrical case, indicating perhaps that including the coupling term between bending and deflection causes further inaccuracies in the calculation.

VI. Conclusions

The Walsh differential operator approach has much to recommend it from the point of view of computational efficiency over other standard methods for determining the interlaminar tractions from finite element displacement data as may be seen from the simplicity of the Fortran routine and the ease with which the nonlinear traction terms may be modeled. The agreement between the Walsh transform method results and those from classical lamination theory has been demonstrated to be excellent for several types of laminates in cylindrical bending.

Acknowledgment

This work has been funded by the Defence Research Agency, Farnborough, England, United Kingdom.

References

[1]Walsh, J., "A Closed Set of Orthogonal Functions," *American Journal of Mathematics*, Vol. 45, 1923, pp. 5–24.

[2]Corrington, M., "Solution of Differential and Integral Equations with Walsh Functions," *IEEE Transactions on Circuit Theory*, Vol. CT-20, No. 5, 1971, pp. 470–476.

[3]Chen, C., and Hsiao, C., "A Walsh Series Direct Method for Solving Variational Problems," *Journal of the Franklin Institute*, Vol. 300, No. 4, 1975, pp. 265–280.

[4]LeVan, T., Tam, L., and Van Houtte, N., "On Direct Algebraic Solutions of Linear Differential Equations Using Walsh Functions," *IEEE Transactions on Circuits and Systems*, Vol. CAS-22, No. 5, 1975, pp. 419–422.

[5]Sannuti, P., "Analysis and Synthesis of Dynamic Systems via Block-Pulse Functions," *Proceedings of the IEE*, Vol. 124, No. 6, 1977, pp. 569–571.

[6]Chen, C., Tsay Y., and Wu, T., "Walsh Operational Matrices for Fractional Calculus and Their Application to Distributed Systems," *Journal of the Franklin Institute*, Vol. 303, No. 3, 1977, pp. 267–284.

[7]Byun, C., and Kapania, R., "Prediction of Interlaminar Stresses in Laminated Plates Using Global Orthogonal Interpolation Polynomials," *AIAA Journal*, Vol. 10, No. 11, 1972, pp. 2740–2749.

[8]Ahner, H., "Walsh Functions and the Solution of Nonlinear Differential Equations," *American Journal of Physics*, Vol. 56, No. 7, 1988, pp. 628–633.

[9]Comlekci, T., "A General Inverse Transformation Method for Isoparametric Elements," private communication, 1995.

[10]Pagano, N., "Exact Solutions for Composite Laminates in Cylindrical Bending," *Journal of Composite Materials*, Vol. 3, 1969, pp. 398–411.

[11]Pagano, N., and Hatfield, S., "Elastic Behavior of Multilayered Bidirectional Composites," *AIAA Journal*, Vol. 10, No. 7, 1972, pp. 931–933.

[12]Guadenzi, P., Barboni, P., and Mannini, A., "A Finite Element Evaluation of Single-Layer and Multi-Layer Theories for the Analysis of Laminated Plates," *Composite Structures*, Vol. 30, No. 4, 1995, pp. 427–440.

Iterative Calculation of the Transverse Shear Distribution in Laminated Composite Beams

J. A. Zapfe* and G. A. Lesieutre†
Pennsylvania State University, University Park, Pennsylvania 16802

Introduction

CLASSICAL lamination theory (CLT) can often be used to accurately predict the stress distribution in beams fabricated from composite materials. However, when the beam is short or when it contains shear soft materials, nonclassical effects such as transverse shear deformation must be considered. One group of beam models that account for transverse shear deformation is known as smeared laminate models (SLMs). SLMs assume a form of the displacement field through the entire thickness of the beam and result in a set of equivalent properties (like the [A], [B], and [D] matrices in CLT) that are used to determine the gross behavior of the beam (e.g., deflection and natural frequency). SLMs that have been presented in the literature lead to constant shear strain, quadratic shear strain, constant shear stress, and quadratic shear stress.[1–6] The limitation of smeared laminate models, when applied to general laminate configurations, is the inherent assumption about the stress distribution that follows from the assumption of the displacement field. If the assumed stress distribution is not representative of the actual stress field, then the smeared laminate model can be significantly in error.

The first SLM that could accurately predict the stress distribution in general laminates was presented by Vijayakumar and Krishna Murty.[7] The authors used an iterative process to successively refine the estimate of the stress/strain field in the laminate. Vijayakumar and Krishna Murty's method produced excellent results when compared with exact solutions. The present SLM is also an iterative method, but unlike Vijayakumar and Kirshna Murty's method, the present model uses the assumed displacement approach of a traditional SLM.

Basic Theory

Consider a beam in which x and u are the in-plane coordinate and displacement, z and w are the transverse coordinate and displacement, and h_u and h_l locate the upper and lower surfaces of the beam. The assumed displacement field over the domain of the beam is

$$\begin{aligned} u(x,z) &= u_0(x) - z\frac{\partial w(x)}{\partial x} + f(z)g(x) \\ w(x,z) &= w(x) \end{aligned} \tag{1}$$

The first two terms in the in-plane displacement expression define the CLT displacement field for a beam. The last term, $f(z)g(x)$, can be thought of as a correction to account for transverse shear effects. The function $f(z)$ represents the shape of the correction through the thickness, whereas $g(x)$ determines its distribution along the beam. The goal of the iterative process is the determination of the function $f(z)$ that makes the stresses and strains self-consistent.

The strain field provides more insight into the nature of the function $f(z)$. Applying the linear strain-displacement relations to Eq. (1) yields

$$\begin{aligned} \epsilon_x(x,z) &= \frac{\partial u}{\partial x} = \frac{\partial u_0}{\partial x} - z\frac{\partial^2 w}{\partial x^2} + f(z)\frac{\partial g}{\partial x} \\ \gamma_{xz}(x,z) &= \frac{\partial u}{\partial z} + \frac{\partial w}{\partial x} = \frac{\partial f}{\partial z}g(x) \end{aligned} \tag{2}$$

From Eq. (2), it can be seen that the gradient $\partial f/\partial z$ represents the shape of the shear strain field through the thickness at a given x location. Therefore, if the shape of the shear strain is known, $f(z)$ can be estimated by integrating the strain through the thickness. In general, $f(z)$ has no closed-form solution. In the present formulation, $f(z)$ is represented numerically as a tabular function.

Static Simply Supported Beams

The present analysis pertains to simply supported beams under a transverse load of the form

$$q(x) = q_0 \sin(kx), \qquad k = n\pi/L \tag{3}$$

where k is the wave number and n is the number of $\frac{1}{2}$ sine waves along the length of the beam.

Whereas the shear correction $f(z)$ changes from iteration to iteration, at any given iteration, $f(z)$ is prescribed and can be treated as a known function. Differential equations of equilibrium and boundary conditions can be developed like any other SLM. The equilibrium equations are

$$\begin{aligned} -K_1u_0'' + K_2w''' - K_3g'' &= 0 \\ -K_2u_0''' + K_4w^{iv} - K_5g''' &= q(x) \\ -K_3u_0'' + K_5w''' - K_6g'' + K_7g &= 0 \end{aligned} \tag{4}$$

and the simply supported boundary conditions, specified at $x = 0$ and $x = L$, are given by

$$\begin{aligned} K_1u_0' - K_2w'' + K_3g' &= 0 \\ K_3u_0' - K_5w'' + K_6g' &= 0 \\ w &= 0 \\ -K_2u_0' + K_4w'' - K_5g' &= 0 \end{aligned} \tag{5}$$

The terms K_{1-7} are section stiffness parameters given by

$$\begin{aligned} K_{[1,2,3,4,5,6]} &= b\int_{h_l}^{h_u} E(z)[1, z, f(z), z^2, zf(z), f^2(z)]\,dz \\ K_7 &= b\int_{h_l}^{h_u} G(z)\left[\frac{\partial f(z)}{\partial z}\right]^2 dz \end{aligned} \tag{6}$$

In the present formulation, the integrals are evaluated numerically using a trapezoidal method.

Functions that satisfy the differential equations and boundary conditions are

$$\begin{aligned} u_0(x) = U_0\cos(kx), \qquad w(x) = W_0\sin(kx) \\ g(x) = G_0\cos(kx) \end{aligned} \tag{7}$$

Received Feb. 28, 1995; presented as Paper 95-1501 at the AIAA/ASME/ASCE/AHS/ASC 36th Structures, Structural Dynamics, and Materials Conference, New Orleans, LA, April 10–12, 1995; revision received Nov. 25, 1995; accepted for publication Dec. 30, 1995.

*Ph.D. Candidate, Department of Aerospace Engineering; currently Research Engineer, Kinetic Systems, Inc., Roslindale, MA 02131. Member AIAA.

†Associate Professor, Department of Aerospace Engineering. Associate Fellow AIAA.